ORIGINAL ARTICLE

Large Inversions Shape Diversification and Genome Evolution in Common Quails

Sara Ravagni[1,2] | Santiago Montero-Mendieta[3] | Jennifer A. Leonard[1] | Matthew T. Webster[4] |
Matthew J. Christmas[4] | Ignas Bunikis[5] | José Domingo Rodríguez-Teijeiro[6] | Ines Sanchez-Donoso[1] | Carles Vilà[1]

[1]Conservation and Evolutionary Genetics Group, Doñana Biological Station (EBD-CSIC), Seville, Spain | [2]Department of Biology and Biotechnologies "Charles Darwin", University of Rome La Sapienza, Rome, Italy | [3]Key Laboratory of Zoological Systematics and Evolution, Institute of Zoology, Chinese Academy of Sciences, Beijing, China | [4]Department of Medical Biochemistry and Microbiology, Uppsala University, Uppsala, Sweden | [5]Uppsala Genome Center, Department of Immunology, Genetics and Pathology, Uppsala University, National Genomics Infrastructure Hosted by SciLifeLab, Uppsala, Sweden | [6]IrBio and Departament de Biologia Evolutiva, Ecologia i Ciències Ambientals, Universitat de Barcelona, Barcelona, Spain

Correspondence: Carles Vilà (carles.vila@ebd.csic.es)

ABSTRACT

Chromosomal inversions, by suppressing recombination, can profoundly shape genome evolution and drive adaptation. In the common quail (*Coturnix coturnix*), a highly mobile bird with a vast Palearctic breeding range, we previously identified a massive inversion on chromosome 1 associated with distinct phenotypes and restricted geographic distribution. Here, using a new *de novo* genome assembly, we characterise this inversion and uncover additional, ancient structural variation on chromosome 2 that segregates across the species' range: either two putatively linked inversions or a single, large inversion that appears as two due to scaffolding limitations. Together, the inversions encompass a remarkable 15.6% of the quail genome (153.6 Mbp), creating highly divergent haplotypes that diverged over a million years ago. While the chromosome 1 inversion is linked to phenotypic differences, including morphology and migratory behaviour, the chromosome 2 inversion(s) show no such association. Notably, all inversion regions exhibit reduced effective population size and a relaxation of purifying selection, evidenced by elevated nonsynonymous-to-synonymous substitution ratios (N/S). This suggests that inversions, particularly the geographically restricted one on chromosome 1, may act as engines of diversification, accelerating the accumulation of functional variation and potentially contributing to local adaptation, especially within isolated island populations. Our findings demonstrate how large-scale chromosomal rearrangements can compartmentalise a genome, fostering distinct evolutionary trajectories within a single, highly mobile species.

1 | Introduction

Chromosomal rearrangements have long captivated scientists for their role in genome evolution. These rearrangements, including variations in chromosome number, translocations, fusions, inversions, and fissions, can influence species diversification by strengthening reproductive barriers (Rieseberg 2001; Brown and O'Neill 2010; Fuller et al. 2019; Höök et al. 2023). From the fusion event in human chromosome 2, where ancestral chromosomes remain distinct in other primates (Yunis and Prakash 1982; IJdo et al. 1991; Poszewiecka et al. 2022), to polyploidy in plant species that fosters genetic redundancy and adaptation (Adams and Wendel 2005; Hufton and Panopoulou 2009), and the multitude of inversions found among *Drosophila* species, likely driving reproductive isolation between sister taxa (Lohse et al. 2015; Sanchez-Flores et al. 2016; Fuller et al. 2019), chromosomal rearrangements are not merely passive bystanders in evolution; they are active players, shaping genomes and driving diversification.

The impact of chromosomal rearrangements extends beyond interspecific divergence and speciation. Within species, many rearrangements, particularly inversions, play a crucial role in maintaining intraspecific diversity (Mérot et al. 2020; Wellenreuther et al. 2019). Inversions can preserve favourable gene combinations, giving rise to supergenes—tightly linked genes or alleles located within a chromosomal region and inherited as a single unit (Thompson and Jiggins 2014). These supergenes can regulate complex traits or phenotypes, facilitating adaptation and evolution (Schwander et al. 2014; Thompson and Jiggins 2014). Indeed, inversions have been found to affect morphological, behavioural, and ecological traits within species, leading to striking phenotypic variation (Wellenreuther and Bernatchez 2018). From mimicry patterns in butterflies (Nishikawa et al. 2015; Jay et al. 2018) and intricate social organisation in ants (Wang et al. 2013; Helleu et al. 2022), to diverse plumage morphs in birds (Lamichhaney et al. 2016; Tuttle et al. 2016) and migratory strategies in fish (Berg et al. 2017; Matschiner et al. 2022), inversions exert a large influence across populations.

Beyond their phenotypic impact, inversions can confer a selective advantage when they capture a set of locally adapted alleles, preventing recombination between advantageous and maladaptive alleles when they are present in a heterozygous state (Kirkpatrick 2010). The suppression of recombination within inversions also leads to reduced genetic variability (Faria et al. 2019). In the early stages of an inversion spread, the derived arrangement may exhibit low genetic variation, but over time, genetic diversity can increase through mutational events and rare instances of recombination involving double crossovers and/or gene conversion (Kirkpatrick 2010; Faria et al. 2019; Korunes and Noor 2019). The maintenance of inversion polymorphisms is often driven by balancing selection, such as overdominance or frequency dependence (Thompson and Jiggins 2014; Wellenreuther and Bernatchez 2018; Faria et al. 2019), facilitating the coexistence of phenotypic variants. However, under divergent selection, inversions can become fixed in certain populations while the ancestral arrangement persists in others, providing a striking example of the intricate interplay between genetic variation and genomic architecture.

The low frequency of recombination events in the inverted region may also lead to the accumulation of deleterious mutations and repetitive elements that escape efficient purging by natural selection over time (Gutiérrez-Valencia et al. 2021). The contrasting recombination rates between inverted and collinear regions lead to disparate rates of deleterious allele accumulation along the genome. Consequently, inversions often exhibit genetic evidence of degeneration, manifested as the accumulation of deleterious mutations, transposable elements, repetitive sequences, and a reduction in genetic diversity and increased gene loss (Gutiérrez-Valencia et al. 2021). Examples of the accumulation of deleterious mutations abound, including inversions governing mimetic coloration patterns in the butterflies *Heliconius numata* (Jay et al. 2021) and *Papilio* (Iijima et al. 2019), as well as those regulating mating behaviour in white-throated sparrows *Zonotrichia albicollis* (Maney et al. 2020). However, certain species do not show significant evidence of degeneration, such as in the inversions influencing social organisation in *Formica* ants (Avril et al. 2020; Brelsford et al. 2020) and in those detected in populations of deer mouse *Peromyscus maniculatus* (Harringmeyer and Hoekstra 2022) and sunflowers (Huang et al. 2022).

The common quail (*Coturnix coturnix*) offers a fascinating case for studying how geographically structured chromosomal variants influence population evolution and sympatric differentiation. In a previous study (Sanchez-Donoso et al. 2022), we identified a massive inversion spanning 115 Mb on chromosome 1 (Chr1) in this small migratory bird. This inversion, encompassing roughly 12% of the quail's genome, is among the largest documented within a species. Surprisingly, despite the vast breeding range—primarily Palaearctic—and high mobility of the common quail, this inversion exhibits a remarkably restricted distribution, seemingly confined to southern regions of the Iberian Peninsula, Morocco, and the Macaronesian Islands. This limited distribution potentially stems from the reduced migratory behaviour observed in quails carrying the inversion (one or two copies). Consequently, this localised inversion creates a scenario where two chromosomal variants coexist, with gene flow homogenising the rest of the genome (Sanchez-Donoso et al. 2022). Thus, the geographically restricted distribution of this inversion serves as a natural experiment, allowing us to investigate how genetic variation and selection act differently on chromosomal inversions compared to the rest of the genome, and how it could contribute to phenotypic diversity within the same population: male quails with the inversion exhibit larger body sizes, differently shaped wings and darker cheek pigmentation. These phenotypic differences might be directly linked to specific ecological pressures within the inversion's restricted range, opening the door to studying the interplay between inversions and local adaptation.

In our prior investigation, we used the Japanese quail (*Coturnix japonica*) genome as a reference. However, the last common ancestor between common quails and Japanese quails occurred approximately 3.3 million years ago (mya; Stein et al. 2015). When species are distantly related or have undergone substantial genomic rearrangements, discerning the boundaries of structural changes becomes challenging. The use of a high-quality reference genome from a more closely related lineage can profoundly improve the characterisation of inversions (Christmas

et al. 2019). Therefore, the first step in characterising chromosomal rearrangements is obtaining an appropriate reference genome for the species under investigation.

In this study, we present a newly assembled reference genome for the common quail, providing a robust foundation for exploring and characterising chromosomal inversions. Using whole genome sequences of 16 quails and genotyping-by-sequencing data of 80, we not only characterised the previously described inversion but also identified additional inversions segregating within the species. We aimed to evaluate the selective forces shaping these inversions and their contribution to local adaptation and diversification within the common quail, thereby broadening our understanding of how geographically restricted inversions influence these evolutionary processes.

2 | Materials and Methods

2.1 | *De Novo* Assembly of a Common Quail Genome

To create a high-quality reference genome for the common quail, we used a male from northeastern Spain previously shown by immunofluorescence to have the ancestral Chr1 gene order (Sanchez-Donoso et al. 2022). Genomic DNA, extracted from a blood sample using a phenol-chloroform protocol and resuspended in TE buffer, was used for long-read data generation at Uppsala Genome Center (National Genomics Infrastructure, SciLifeLab Genomics Platform, Sweden) on two PacBio Sequel II SMRT cells. The genome was assembled with Hifiasm v. 0.16.0 (Cheng et al. 2021, 2022) combining HiFi reads (16X coverage) with systematically filtered non-HiFi reads (minimum length of 5 kbp, at least 1 pass and predicted accuracy above 0.9), yielding 22X total coverage (see Results). While this coverage was sufficient for assembly, it limited our ability to remove duplicate regions and to perform a comprehensive assembly assessment. We used BlobTools2 (Challis et al. 2020) to test for the presence of contaminants, and we ran BUSCO v. 5.2.2 using the avian dataset "aves_odb10" to assess the presence and contiguity of avian-specific genes. Scaffolding into chromosomes was done based on the Japanese quail genome (RefSeq assembly accession number: GCF_001577835.2) using RagTag v2.1.0 (Alonge et al. 2022) and we transferred the annotation using Liftoff (Shumate and Salzberg 2021). We assessed structural differences between the Japanese quail genome and the new common quail assembly using CHROMEISTER (Pérez-Wohlfeil et al. 2019), which aligns the two sequences and generates a dotplot of potentially homologous sequences.

2.2 | Identification of Chromosomal Rearrangements Within Common Quail

We aligned sequences both to our newly assembled *Coturnix coturnix* genome and the Japanese quail genome, building on data from Sanchez-Donoso et al. (2022). This analysis included whole-genome resequencing (WGS) data from 16 male common quails (GenBank accession code: PRJNA730394), sequenced at a coverage of about 10× using Illumina HiSeqX (2×150bp), and genotyping-by-sequencing (GBS; Elshire et al. 2011) data from

80 adult males (data available at Digital.CSIC, https://doi.org/10.20350/digitalCSIC/13989), with a mean coverage depth of 25×. The samples originated from multiple locations across the Iberian Peninsula, Italy, Morocco, and the Macaronesian archipelagos of the Canary Islands and Madeira. GBS data was obtained after digestion with the restriction enzyme EcoT22I and sequenced using Illumina HiSeq 2500 (1×100bp). Importantly, for WGS samples, we specifically selected only homokaryotypes for the Chr1 inversion.

For WGS data, we mapped reads to the *de novo* assembly of the common quail genome using BWA-MEM v.0.7.15 (Li and Durbin 2009). We performed read group tagging and duplicate marking with PICARD v.2.4.1 (https://broadinstitute.github.io/picard/) and used GATK v3.6 (McKenna et al. 2010) for joint indel realignments. We called SNPs using FreeBayes v.1.3.1 (Garrison and Marth 2012) and applied filters as in Sanchez-Donoso et al. (2022). Briefly, we filtered the VCF file by quality and depth, retaining SNPs located on chromosomes with less than 50% missing data, minor allele count >2, mapping quality higher than 40, and a mean depth lower than 30X. In total, 25,245,046 biallelic SNPs were retained. For GBS data, we called variants using the Tassel5 GBS v.2 pipeline (Glaubitz et al. 2014) and we mapped the reads using bowtie2 v.2.4.1 (Langmead and Salzberg 2012). We kept biallelic SNPs with minor allele frequency greater than 0.03, missing data less than 25%, and depth greater than 5X and lower than 100X using VCFTOOLS v.0.1.13 (Danecek et al. 2011). After applying these filters, a total of 51,024 biallelic SNPs were retained for analysis.

To identify potential chromosomal inversions segregating within our data, we carried out principal component analyses (PCAs) in sliding-windows of 50, 100 and 200 kbp along the 16 quail genome sequences using the SNPRelate R package v. 1.30.1 (Zheng et al. 2012) with the scripts of Jay et al. (2021); https://github.com/PaulYannJay/Mutation-load-analysis. Large inversions are expected to produce PCA representations that consistently form clusters with the same individuals, with homokaryotypes clustering at opposite extremes along the first principal component. We plotted the results with the package ggplot2 v.3.4.1 (Wickham 2009) in R 4.2.1 (R Core Team 2022) using RStudio v.2022.07.1 (RStudio Team 2022). This allowed us to observe the inversion in Chr1 found by Sanchez-Donoso et al. (2022) as well as other inversions. We then calculated the average F_{ST} between the two groups of homokaryotype individuals for the inversions across non-overlapping 1 kbp and 1000 kbp windows using VCFTOOLS. We also assessed mappability using GenMap v.1.2.0 (Pockrandt et al. 2020), allowing up to 3bp mismatches in 150bp k-mers, and we computed average mappability in 1 Mbp non-overlapping windows to identify regions of low mappability. Finally, we plotted F_{ST} and mappability values along the chromosomes of interest with the package ggplot2.

To determine the genotype of each individual for the potential inversions, we extracted the variable sites within the potentially inverted regions using VCFTOOLS and also from the same region in the GBS database. We performed population structure analyses based on the variable sites within each of the putative inversions for WGS and GBS data using ADMIXTURE v.1.3.0 (Alexander et al. 2009). We set the number of clusters (*K*) to 2. This program estimates the proportion of the genome derived

from each one of the two clusters for a region for each individual. If an inversion exists, homokaryotypes should belong to just one cluster, while heterokaryotypes should be an approximate 50:50 mix of the two clusters. We ran 20 independent runs with default parameters to evaluate potentially cryptic substructure. We compared the results of the different runs using the CLUMPAK server (Kopelman et al. 2015). To assess the suppression of recombination in the inverted regions, we thinned the SNP dataset for sites at a minimum distance of 50 kbp and we calculated R_2 values in Chr2 with the LDHeatMap package (Shin et al. 2006) in R for all homokaryotypes and only for inverted and non-inverted samples.

To investigate the presence of repetitive sequences at the inversion breakpoints, we first identified their approximate position by analysing PCA and F_{ST} plots, identifying the transition in F_{ST} values. These positions were inferred to be within the regions showing genetic divergence, acknowledging that the effects of genetic hitchhiking may extend the apparent boundaries of divergence beyond the actual breakpoints. We carried out pairwise alignments between regions including the potential breakpoint positions using the online version of the sequence aligner MAFFT v.7 (https://mafft.cbrc.jp/alignment/server/; Katoh and Standley 2013). We assessed the repeat content of these regions by running RepeatMasker with default parameters and setting the query species as vertebrata metazoa (https://www.repeatmasker.org/cgi-bin/WEBRepeatMasker; Smit et al. 2013).

To compare the divergence time of the inversion haplotypes, we calculated their absolute genetic divergence (d_{XY}). We used the script from Sanchez-Donoso et al. (2022); https://github.com/MattChristmas/Quail_inversion_scripts on the first and last 2 Mbp of the inverted region, because the divergence along large inversions could be different due to double crossovers within the inversion. Thus, the largest divergences are expected to be around the breakpoints. We masked genic regions to focus on neutral evolutionary processes, thereby reducing the impact of selective forces on the divergence estimates. We estimated the divergence time based on the equation: $T = d_{XY}/(2*\mu)$, where T is the divergence time in generations and μ the mutation rate in mutations per site per generation. We used mutation rates estimated for other bird species as in Sanchez-Donoso et al. (2022), i.e., for the ancestral bird lineage (1.23×10^{-9} site^{-1} generation^{-1}), chicken (1.91×10^{-9} site^{-1} generation^{-1}), zebra finch (2.21×10^{-9} site^{-1} generation^{-1}) from Nam et al. (2010), and collared flycatcher (4.6×10^{-9} site^{-1} generation^{-1}) from Smeds et al. (2016). Since generation time in common quails is estimated to be about 1 year (Puigcerver et al. 1992), divergence time estimates in years correspond to the number of generations.

2.3 | Estimation of Selective Forces Within the Inversions

We calculated individual heterozygosity for different genomic regions using VCFTOOLS. To estimate the recent effective population size for the different chromosomal variants at the inverted regions, we used the software GONE (Santiago et al. 2020). We ran 40 independent analyses in GONE using default parameters except for the recombination rate, which was assumed to be 3.295 cM/Mb (Ravagni et al. 2024). Because estimates for the

last 5 to 10 generations are less reliable due to fewer recombination events, we estimated the current effective population size as the average between 10 and 30 generations ago.

We generated VCF files for each individual and for groups of individuals (homokaryotypes with/without inversion) using BCFtools v.1.10.2 (Li 2011; Danecek et al. 2021) and identified synonymous and nonsynonymous substitutions within the genes. To predict the potential functional impact of these substitutions, we utilised the Ensembl Variant Effect Predictor (McLaren et al. 2016). For this analysis, we used the variant file generated by mapping the sequences to the Japanese quail reference genome (RefSeq assembly accession number: GCF_001577835.2) and its associated annotation. Due to the unavailability of a *de novo* common quail genome annotation and potential inaccuracies in annotation transfer, the Japanese quail reference provided a more reliable framework to assess variant effects and avoid uncertainties that could influence reading frame predictions. Next, we estimated the ratio of nonsynonymous to synonymous variants (N/S) in the regions with inversions for all samples by comparing their sequence to the reference genome. Finally, we performed a Wilcoxon signed rank test in R using the function wilcox.test() from the rstatix package to test whether the values of the missense/synonymous substitution ratios (N/S) were significantly different between chromosomal variants.

For all protein-coding genes in the inverted regions, we conducted Gene Ontology (GO) enrichment tests for the categories of Biological Process, Cellular Component, and Molecular Function using ShinyGO v0.77 (Ge et al. 2020) with a FDR cutoff of 0.05. The presence of enriched pathways could inform about the evolutionary significance of the inversions and their potential role in local adaptation. To look for evidence of selection in the regions, we identified protein-coding genes that included ≥ 1 synonymous and ≥ 1 nonsynonymous variants in inverted and non-inverted haplotypes. We then calculated the N/S ratio for each gene and the difference in this ratio between inverted and non-inverted haplotypes. We extracted information on the function of genes that showed a difference of more than 0.5 in the N/S ratio between the two chromosomal variants using the BioMart database (https://www.ensembl.org/biomart/martview) selecting the attribute "GOSlim GOA Description". The 0.5 threshold was chosen based on the distribution of the differences in N/S ratio among genes (see results).

We also looked for regions in the inverted and non-inverted haplotypes that might have particularly low or high coverage along windows. This could be an indication of duplicated regions or indels that could reflect degeneration. We calculated the mean individual depth along the inversion regions using the bedcov function of SAMtools v.1.10 (Danecek et al. 2021) in windows of 10,000 bp. We generated the windows along the genome using makewindows from BEDtools v2.27.1 (Quinlan and Hall 2010). To detect differences in depth between individuals with and without the inversions when not all individuals were sequenced to the same coverage, we normalised the depth of coverage of each window by dividing it by the individual mean depth for the entire inversion region in that individual. We tested whether the means of the normalised values were different between individuals with and without the inversion by performing a Wilcoxon

signed rank test. We chose a non-parametric test because of the deviations from normality.

2.4 | Evaluation of Phenotypic Effects Associated with the Inversions in Chr2

We examined the association between inversion karyotype and several phenotypic traits (see Sanchez-Donoso et al. 2022 for details on the measurements) in 75 1-year-old males (we excluded five 2-year-old males to avoid possible variance due to age): weight, tarsus length (indicators of body size), weight/tarsus length (a proxy for body condition, Labocha and Hayes 2012), wing length, a modified Holynski index (which accounts for wing pointedness, related to flight efficiency), width of the lateral lipid band (fat accumulation that is larger in birds preparing for migration), cloacal aperture width (larger in sexually active birds), beak length, beak height, and beak width (related to food specialisation). We fitted a linear model for each one of the response variables by using karyotype as the explanatory variable. Homoscedasticity and normality of the residuals were checked by visual inspection of the scatterplots, and both were fulfilled. Significance was evaluated with an *F*-test using the Anova() function available in the R package car. We tested the effect of karyotype on cheek pigmentation (classified from 1, fair, to 6, completely dark) with a Fisher exact test using the fisher.test() function in R v. 4.2.3 (R Core Team 2022) and RStudio v. 2023.03.0 (RStudio Team 2023).

3 | Results

3.1 | *De Novo* Assembly of a Common Quail Genome

We sequenced long PacBio reads from a male common quail and obtained 16.4 Gbp HiFi data (19 kbp mean read length, 16X coverage) and 6.1 Gbp non-HiFi reads (quality values < 20, 19.5 kbp average length), resulting in 22X total coverage. The assembled genome consisted of 1584 contigs (78% > 50,000 bp, N50 = 2.5 Mb), with a total length of 1.08 Gb. Of these, 88% (784 contigs, adding to 0.95 Gb) were located on 31 Japanese quail chromosomes. The chromosomal portion of our assembly is approximately 3.6% larger than the Japanese quail genome. The comparison of the two quail genomes suggested the presence of small chromosomal inversions or rearrangements in chromosomes 1, 2, and 5, but we did not observe large structural changes (Figure S1). We also did not detect any sequence located in different chromosomes in the two species, although it is worth noting that several fragments were not placed within chromosomes. Nonetheless, the detection of interspecific rearrangements may be limited due to the scaffolding based on the Japanese quail genome and this representation is likely to underestimate the presence of large structural differences between the two genomes. The BUSCO analysis indicated that the assembly included 96% of complete single-copy orthologs for conserved avian genes, with 98.8% classified as single-copy and 1.2% as duplicated. Fragmented orthologs accounted for 0.7%, while missing orthologs comprised 3.1%. The unplaced contigs accounted for 128 Mbp and contained highly repetitive sequences. Although these contigs did not yield significant Blast hits, they included

57 additional conserved genes (0.07%). Mapping the annotated genes from the Japanese quail genome allowed us to identify 15,186 protein-coding genes (14,799 located on chromosomes), compared to 15,719 in the Japanese quail genome.

3.2 | Polymorphic Chromosomal Rearrangements Within the Common Quail

We used the sliding-window PCA approach to compare the genomes of 16 male common quails mapped to the new genome assembly and confirmed the presence of the previously described inversion in Chr1 (Figure S2; Sanchez-Donoso et al. 2022). To investigate the presence of repetitive regions at the breakpoints that may indicate nonallelic recombination events as the origin of the inversion, we aligned 100 kbp sequences flanking these regions, estimated to be located around coordinates 52,800,000-52,860,000 and 170,250,000-170,270,000 (Figure S3A). This alignment revealed that approximately 13.57% of these regions were composed of repetitive or low complexity elements, predominantly LINE elements of the L3/CR1 type (86%), compared to 7.23% of LINE elements in the entire chromosome. The absence of a long-read assembly from a quail carrying the inversion limits the ability to pinpoint the locations of the breakpoints with greater precision. We estimated that the inversion in Chr1 (hereafter referred to as Inv1) encompassed nearly 117.5 Mbp (i.e., 12.3% of the genome) and contained 1213 protein-coding genes (8.2% of the total).

The combined use of sliding-window PCA, analyses of differentiation between the identified groups (measured as F_{ST}), and linkage disequilibrium (LD) allowed us to identify new putative structural variants (Mérot et al. 2020). The PCA analyses suggested the presence of two additional large inversions in Chr2 (Figure 1A). Comparison between two groups of individuals, each consisting of four apparent homokaryotypes, revealed strong genetic differentiation in these regions (Figure 1B) and high LD (Figure 1C) within each region. Moreover, heterokaryotypes exhibited higher levels of heterozygosity within the inverted regions, a characteristic feature of inversions (Figure 2). Further PCA analyses of SNPs within these regions conducted on a larger set of 80 quails genotyped with GBS confirmed the differentiation into the same three distinct groups (Figure S4). We named these putative inversion regions Inv2.1 and Inv2.2.

To assign genotype to each individual, we performed ADMIXTURE analyses on SNPs located within the potential inverted regions. We assumed two ancestral clusters ($K = 2$) and carried out this analysis on both the WGS data from 16 individuals and the GBS data from the larger sample of 80 individuals. The results revealed a distinct pattern: individuals either carried markers exclusively from one of the two inferred ancestral groups (homokaryotypes), or displayed a balanced (approximately 50:50) combination of both, indicative of heterokaryotypes. Interestingly, each individual consistently displayed the same karyotype across both regions (Figure 3). Furthermore, LD analyses showed strong linkage between the two putative inversions, despite their separation by an approximately 25 Mbp intervening sequence (Figure 1C). The WGS and GBS karyotypes (individuals typed for GBS included those typed for WGS) revealed 4 (WGS) and 26 (GBS) homokaryotypes
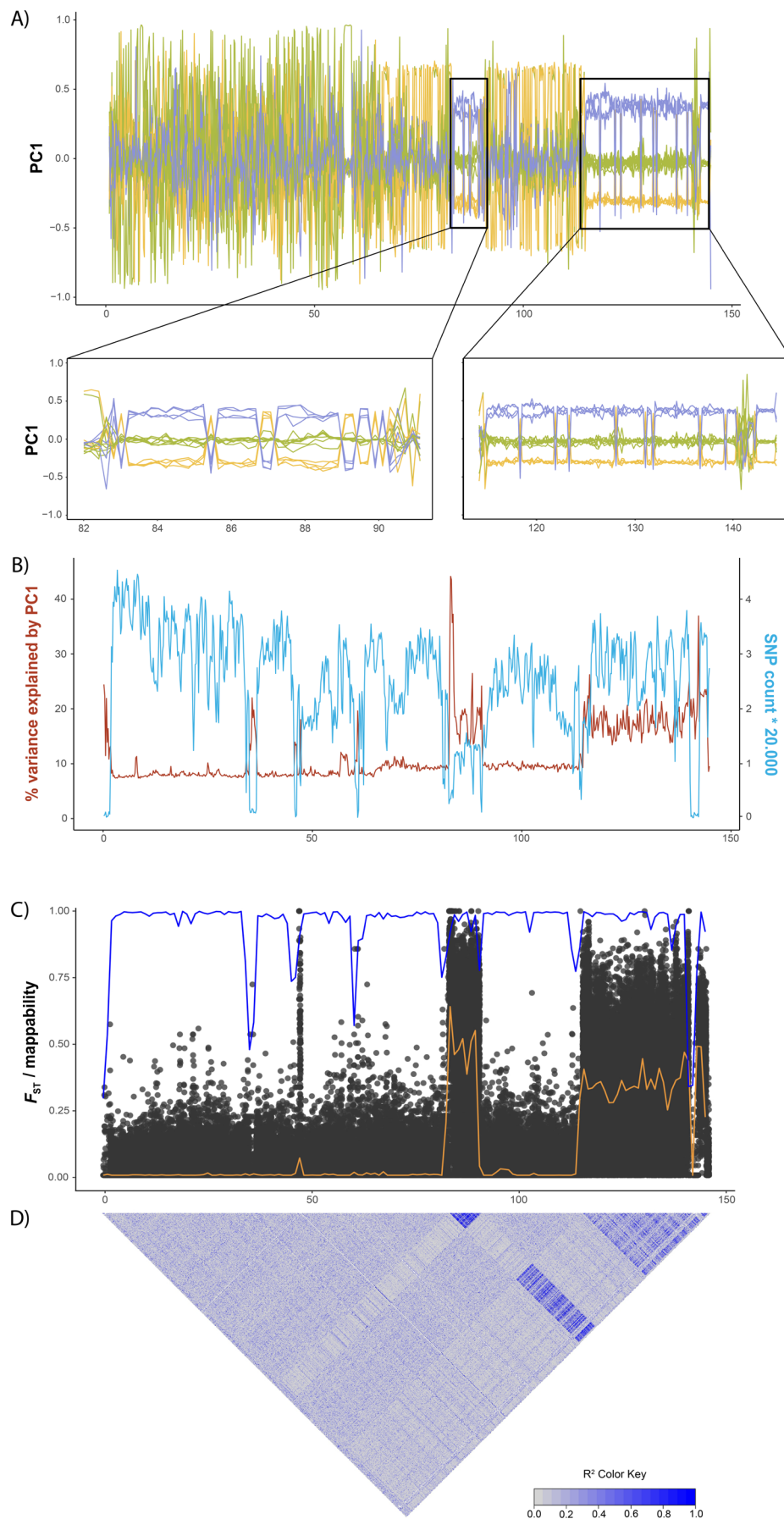
FIGURE 1 | Legend on next page.

FIGURE 1 | Variation along Chr2 in 16 common quails. (A) PCA in sliding-windows of 200 kbp. Each line represents the position of one individual on the first principal component. When an inversion is present, three differentiated groups can be observed: Homokaryotypes for the inversion or with the ancestral order (top and bottom, marked in purple and orange) and heterokaryotypes (middle, in green). This shows the presence of two putative inversions, labelled Inv2.1 and Inv 2.2. (B) Variance explained by PC1 (%) for the sliding-windows PCAs represented in panel A, and SNP count for each window. (C) Manhattan plot comparing F_{ST} values along Chr2 in 1-kbp windows for the two groups of individuals separated as potential homokaryotypes in panel A. The orange line represents F_{ST} values in 1-Mbp windows, while the blue line indicates the mappability scores in the same windows. The sequences at the putative inversions are very differentiated. (D) Linkage disequilibrium (LD) heatmap along Chr2 considering only homokaryotypes for the two putative inversions. Blue regions indicate higher LD, showing high linkage between the two regions. [Colour figure can be viewed at wileyonlinelibrary.com]
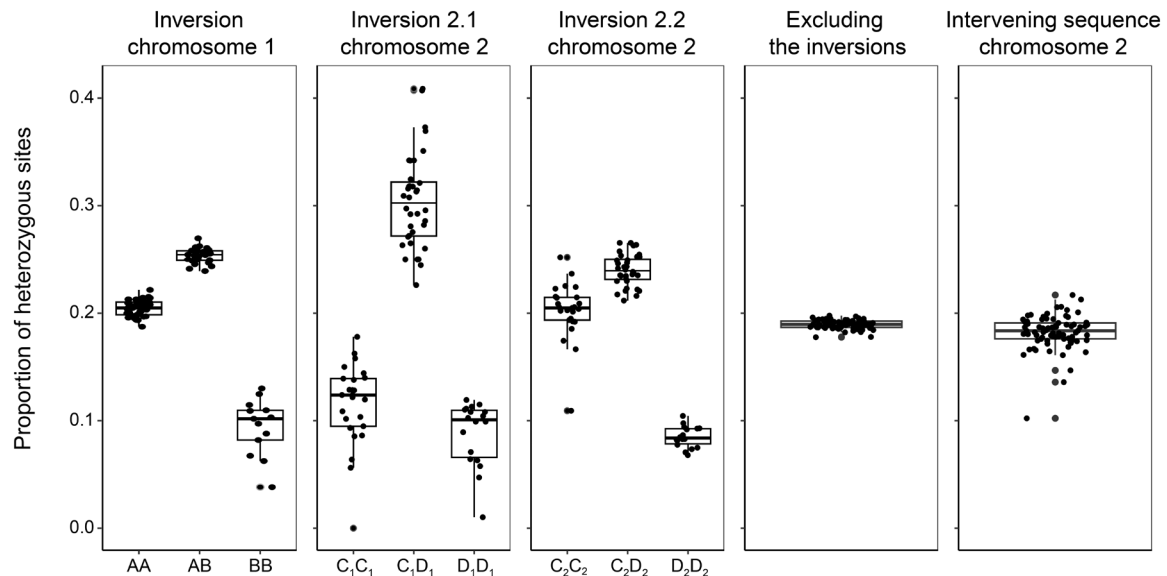

FIGURE 2 | Individual heterozygosity across Inv1, Inv2.1, Inv2.2, across the rest of the genome and for the intervening sequence that separates Inv2.1 and Inv2.2 for the karyotype groups obtained from GBS data. For two of the inversions (Inv1 and Inv2.2), one of the homokaryotypes has very low heterozygosity compared to the other or to the rest of the genome. For Inv2.1, heterozygosity is reduced for both homokaryotypes.
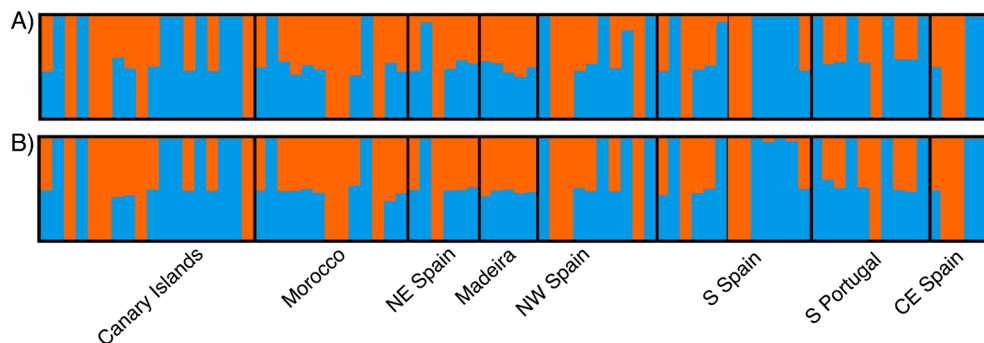

FIGURE 3 | ADMIXTURE plot for $K=2$ for the two inverted regions in Chr2 for 80 male common quails genotyped with GBS. (A) Inv2.1, from position 83,000,000 to 90,000,000; (B) Inv2.2, from position 115,000,000 to 144,300,000. All individuals cluster in the same groups for both inversions, suggesting linkage between the two inversions. [Colour figure can be viewed at wileyonlinelibrary.com]

for one chromosomal variant (hereafter referred to as C_1C_1 for Inv2.1 and C_2C_2 for Inv2.2), 4 and 18 homokaryotypes for the other (D_1D_1 and D_2D_2), and 8 and 36 heterokaryotypes (C_1D_1, C_2D_2). The quail used for the de novo assembly was genotyped as AA for Inv1 based on immunofluorescence assays (Sanchez-Donoso et al. 2022) and clustered together with D_1D_1 and D_2D_2 for Inv2.1 and Inv2.2.

To explore whether the intervening sequence separating the two inversions in chromosome 2 exhibited differentiation similar to

the inversion regions, we performed an ADMIXTURE analysis for markers in this region. The results from the 80 individuals studied with GBS did not reveal distinct clusters (Figure S5), suggesting that Inv2.1 and Inv2.2 were co-inherited while the intervening region exhibited a different inheritance pattern. The identical karyotype patterns and strong linkage disequilibrium for Inv2.1 and Inv2.2 (Figures 1C and 3), despite being separated by a region lacking population structure, raise the question of whether these represent two distinct inversions or a single, larger inversion. While our *de novo* assembly, scaffolded against the

Japanese quail genome, suggests two separate regions, it is possible that this is an artefact of the scaffolding process. A large rearrangement has occurred within Chr2 differentiating common and Japanese quail (see Kartout-Benmessaoud et al. 2024) and, as a result, contiguous regions in the common quail Chr2 could appear separated when mapped against the Japanese quail and an inversion could appear as two. Alternatively, strong selection on co-adapted alleles within two closely linked inversions could, in principle, lead to the observed pattern of complete linkage. We attempted to address this possibility by searching for long reads spanning the putative breakpoints (Figure S6), but the imprecise breakpoint locations limited our ability to draw firm conclusions. Given this uncertainty, and taking into account the large differences in selective forces between the putative inversions (see below), we continue to refer to the regions as Inv2.1 and Inv2.2 throughout the manuscript.

We estimated the breakpoints of these two regions in our *de novo* assembly to be located between positions 83,000,000-83,200,000 and 89,800,000-90,000,000 for Inv2.1 and 114,900,000-115,050,000 and 144,200,000-144,300,000 for Inv2.2. These resulted in lengths of 6.8 Mbp and 29.3 Mbp, respectively, constituting 0.7% and 2.6% of the assembled genome. These inversions contained a total of 75 and 213 genes, accounting for 0.5% and 1.4% of the total gene count. Subsequently, we aligned 100 kbp sequences around the breakpoints to identify potential homologous regions (Figures S3B,C). Analysis of the repeat content within these regions revealed that approximately 13.4% for Inv2.1 and 18.6% for Inv2.2 consisted of highly repetitive sequences, with LINE elements being the most abundant. Among these, L2/CR1/Rex elements predominated, comprising 66% and 75% of the repetitive sequences at the breakpoints. Additionally, the regions included a mix of simple repeats and Long Terminal Repeat (LTR) elements. Overall, LINE elements accounted for 6.3% of Chr2.

The absolute divergence (d_{XY}) was 0.0164 for the two groups of homokaryotypes for Inv1 (comparison of AA and BB individuals), 0.0171 for Inv2.1 (C_1C_1 vs. D_1D_1) and 0.0133 for Inv2.2 (C_2C_2 vs. D_2D_2), giving minimum divergence times of 1.8, 1.9 and 1.4 mya, respectively. However, these are very rough estimates. If diversity in the ancestral population was much larger or smaller than in the contemporary populations, the divergence would be biased upwards or downwards, respectively. For Inv1 we obtained a higher divergence than previously reported (0.0079; Sanchez-Donoso et al. 2022). This discrepancy in divergence values is likely due to the use of different reference genomes. Mapping data to the more distant Japanese quail genome hampers mapping efficiency and consequently reduces the number of identified variants (Bohling 2020).

Alongside the two large inverted regions in Chr2, we also observed a peak of high F_{ST} around position 47,000,000 (46,850,000 to 47,300,000; Figure 1B). This peak contained 6 genes and our ADMIXTURE analyses (16 quails, WGS data) showed a segregation pattern similar to Inv2.1 and Inv2.2, suggesting that they segregate together (Figure S7). However, due to potential scaffolding issues in this region (indicated by the lower mappability, Figure 1B) we cannot confirm this F_{ST} peak as an independent inversion event. Additionally, we identified potential smaller inversions (< 5 Mbp) scattered across several other chromosomes.

Due to the limited sample size, most of these smaller inversions were only observed in a single individual. Their small size and low SNP density in the GBS dataset make further characterisation challenging in this study.

3.3 | Geographic Distribution and Phenotypic Effects of the Inversions

Unlike the inversion on Chr1 (Inv1), which seems to be confined to the western edge of the quail's distribution (southern Iberian Peninsula, Morocco and Macaronesian archipelagos; see Sanchez-Donoso et al. 2022), the putative inversions on Chr2 (Inv2.1 and Inv2.2, or the potentially single larger inversion) were found throughout the sampled range, including also northern Spain and Italy (Figure S8).

Previously, we reported strongly significant phenotypic differences between quails with and without the inversion for Inv1 (haplotype B; Sanchez-Donoso et al. 2022). These differences even extended to isotopic signatures in feathers grown during breeding and wintering seasons, suggesting distinct migratory behaviours. However, for Inv2.1 and Inv2.2, no significant associations were found between karyotype and the phenotypic traits we measured: weight: $F_{2,72} = 0.644$, $p = 0.528$; tarsus length: $F_{2,71} = 0.047$, $p = 0.954$; weight/tarsus length: $F_{2,71} = 0.848$, $p = 0.432$; wing length: $F_{2,66} = 1.956$, $p = 0.150$; modified Holynski Index: $F_{2,46} = 0.857$, $p = 0.431$; width of the lateral lipid band: $F_{2,72} = 0.432$, $p = 0.651$; beak length: $F_{2,34} = 0.298$, $p = 0.744$; beak height: $F_{2,36} = 0.095$, $p = 0.909$; beak width: $F_{2,35} = 0.062$, $p = 0.940$; cheek pigmentation: Fisher's exact test, $p = 0.132$; cloacal aperture width: $F_{2,65} = 0.538$, $p = 0.587$ (Figure S9).

3.4 | Selective Forces Within the Inversions

We observed large differences in heterozygosity within the inverted regions for the different karyotype groups (Figure 2). In the case of Inv1 and Inv2.2, a similar pattern emerged: one homokaryotype (AA for Inv1, C_2C_2 for Inv2.2) displayed heterozygosity slightly exceeding that seen in the collinear genome and the intervening sequence on Chr2 (mean heterozygosity: AA, 0.205; C_2C_2, 0.202; collinear, 0.189; intervening, 0.182); the other homokaryotype had very much lower heterozygosity (BB, 0.094; D_2D_2, 0.085) and heterokaryotypes had, as expected, higher heterozygosity (AB, 0.253; C_2D_2, 0.240). On the other hand, the pattern was very different for Inv2.1, with low heterozygosities for both homokaryotypes (C_1C_1, 0.115; D_1D_1, 0.088), and very high for heterokaryotypes (C_1D_1, 0.304). We estimated effective population size (N_e) for the haplogroups by considering polymorphic positions in homokaryotype individuals. Our findings indicate that the estimated N_e was several thousand individuals in all cases except for BB homokaryotypes, which exhibited a considerably lower effective population size ($N_e = 355$).

We used the nonsynonymous to synonymous substitution ratio (N/S) as a metric to evaluate selective pressures acting within the chromosomal inversions. This assessment was based on variants identified using the Japanese quail genome as a reference due to the unavailability of a precise annotation for the common quail, which hindered the accurate transfer of reading frames. The N/S
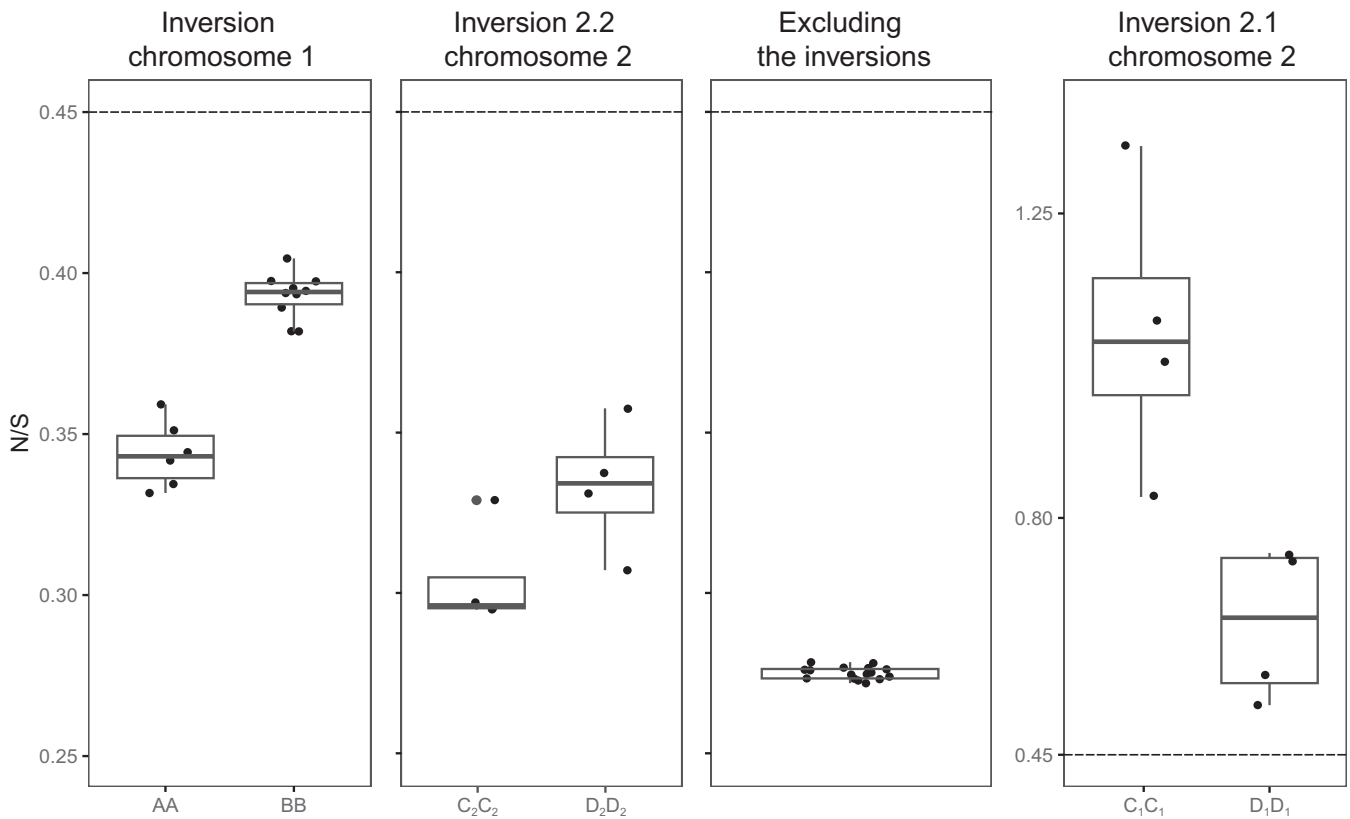
FIGURE 4 | Distribution of individual N/S ratios for homokaryotype individuals for each different chromosomal inversions and for the rest of the genome. Increased N/S values in the inverted regions in relation to the rest of the genome is compatible with a relaxation of selective forces. Note that the y-axis for Inv2.1 has a different scale and the ratios are very much higher (a dotted line at N/S = 0.45 is marked as reference).

value was consistently lower in the non-inverted regions (collinear genome) compared to all inverted regions (mean for the collinear genome = 0.275; $p < 0.001$ in all comparisons). Within Inv1, the N/S ratio was significantly higher for quails with the inversion (mean for AA = 0.344; for BB = 0.393; $p < 0.001$, Figure 4). For Inv2.2, values were similar to those observed for Inv1 (mean for C_2C_2 = 0.304; for D_2D_2 = 0.333; $p = 0.057$), although the difference between haplogroups did not reach statistical significance, likely due to the smaller sample size. In contrast, both genotypes in Inv2.1 exhibited exceptionally high N/S ratios, with a significant difference despite the limited sample size (mean for C_1C_1 = 1.075; for D_1D_1 = 0.644; $p = 0.029$).

We explored enriched pathways for protein-coding genes within each inverted region using Gene Ontology (GO) terms. While Inv1 displayed significantly enriched pathways in the Molecular Function category (Interleukin-1 receptor activity and UDP-glucosyltransferase activity; Table S1), no pathways were enriched for Inv2.1, and only one (Carbonate dehydratase activity) was found in Inv2.2. To identify genes potentially under selection within the inversions, we examined those containing SNPs leading to both synonymous and nonsynonymous substitutions with a difference greater than 0.5 in the N/S ratio between inverted and non-inverted haplotypes, a threshold determined based on the N/S distribution (Figure S10). This revealed 111 genes in Inv1, 11 in Inv2.1, and 20 in Inv2.2 exceeding the threshold (Tables S2–S4). Interestingly, all 11 genes in Inv2.1 had N/S differences exceeding 1, while less than half of the genes in Inv1 (50 out of 111) and 40% in Inv2.2 (8 out of 20) reached such high

differences. This suggests potentially stronger selection pressures acting on genes within Inv2.1.

We further analysed the functional roles of genes with the largest N/S discrepancies. In Inv1 (Table S2), these genes were involved in diverse roles like anatomical development, cell differentiation, organelle functions, reproduction, and signalling. Inv2.1 (Table S3) mirrored some functions seen in Inv1 but also included protein modification and enzymatic processes. Genes in Inv2.2 (Table S4) were associated with lipid metabolism, cell division, DNA repair, and chromosome organisation. Interestingly, across all inversions, a trend emerged: genes with high N/S ratios were most prevalent for organelle functions, followed by those involved in catalytic activity and the nucleus (Table S5). Notably, genes related to anatomical development were also important, making it the fourth most prevalent GO term.

Limited recombination within inversions can result in the accumulation of repetitive elements or lead to gene loss. This can result in apparent differences in coverage depth when comparing whole genome sequences of individuals with and without the inversion. For Inv1, when significant differences in coverage were observed between the two haplotypes, the depth was generally larger in individuals not carrying the inversion (karyotype AA; 808 out of 907 windows with differences in coverage). However, most differences between the mean standardised depth values for non-inverted and inverted haplotypes were less than 0.5 (mean coverage per bp less than 50% higher for one group

than for the other). This suggests the insertions/deletions likely only affected short stretches of DNA. Only 28 non-contiguous windows showed higher values, with a maximum difference of 1.36. These findings point towards a widespread loss of small genomic fragments within the inverted sequence of Inv1. In contrast, no significant depth variations were observed for the Chr2 inversions. However, our limited sample size (only four homokaryotypes of each type) might be insufficient to detect such differences.

4 | Discussion

The rise of long-read sequencing technologies has fueled a surge in newly assembled genomes. This reduces dependence on genomes from other species as references, leading to a deeper understanding of genome evolution and population genomics. In this study, our *de novo* assembly of the common quail genome was crucial for identifying and characterising chromosomal rearrangements segregating within this highly mobile bird species. While generally syntenic with the Japanese quail genome, our assembly reveals a slightly larger total chromosomal length. This discrepancy likely stems from a combination of factors. First, numerous small variations scattered throughout the genome, rather than a single large region, might contribute to the increased size. Second, the moderate sequencing coverage limited our ability to remove duplicate regions, potentially leading to an overestimation of the genome size. Finally, our assembly captures only 31 chromosomes, whereas the common quail karyotype has 39 pairs (Kartout-Benmessaoud and Ladjali-Mohammedi [2018]). The 128 Mbp of unplaced, highly repetitive sequences likely reside, at least in part, on these unassembled chromosomes. Therefore, both our assembly and the previously published Japanese quail assembly likely underestimate the true total genome length.

Our genome assembly aligns with the prevailing view of a high degree of conservation in avian genomes, particularly in terms of chromosome number and rearrangements within *Galliformes* (Dalloul et al. [2010]; Morris et al. [2020]). The common and Japanese quails, which diverged approximately 3.3 mya (Stein et al. [2015]), exhibit only minor changes in gene order and small inversions on three chromosomes when their genomes are compared (Figure [S1]). This low structural variation is consistent with findings from the comparison of the chicken and Japanese quail genomes, which, despite diverging around 40 mya, only showed 33 rearrangements (Stein et al. [2015]). However, the number of large chromosomal rearrangements in *Coturnix* quails is likely to be underestimated by the use of the Japanese quail genome for scaffolding our common quail genome. Putative inversions which appear separate in our alignment may indeed correspond to a single large inversion segregating in common quails if there have been other chromosomal rearrangements between common and Japanese quail. Considering the conserved synteny in *Galliformes* chromosomes, the identification of multiple large inversions within quail species and populations is both unexpected and intriguing, raising questions about their potential role in quail evolution and adaptation.

In a previous investigation, we found a large inversion in Chr1 associated with morphological and behavioural polymorphisms within populations at the western edge of the common quail distribution range (Sanchez-Donoso et al. [2022]). Our current study identifies two new inverted regions in chromosome 2. Notably, these two putative inversions, Inv2.1 and Inv2.2, display a consistent pattern of cosegregation across all studied individuals, confirmed by a strong linkage between the two regions. As indicated above, these two inversions could be an artefact associated with the use of the Japanese quail genome for scaffolding and represent a single large inversion. However, the complete linkage disequilibrium between these inversions could also be explained by strong selection on co-adapted genes. Cosegregating inversions have been previously documented by Lundberg et al. ([2023]) in willow warbler, *Phylloscopus trochilus*, where cosegregation was attributed to selective forces arising from differences in migratory behaviour. This scenario could account for the observed low diversity in the two Inv2.1 homokaryotypes (Figure [2]), likely resulting from genetic hitchhiking. In any case, the inverted regions of the genome in Chr2 include an additional 3.3% of the common quail genome. The breakpoints of these two inversions coincide with chromosomal regions with a higher concentration of the same LINE elements, L2/CR1/Rex, which could have facilitated nonallelic homologous recombination (Cáceres et al. [1999]; Gray [2000]; Hedges and Deininger [2007]). The identification of new inversions, coupled with the potential presence of additional rearrangements within the common quail genome, highlights the important role that structural variations may play in driving evolutionary processes in this species.

The identified chromosomal inversions differ in terms of size, geographic distribution, associated phenotypic effects, and effective population size. Inv1 has been found to be associated with changes in morphology and migratory behaviour, and has a limited geographical distribution (Sanchez-Donoso et al. [2022]). In contrast, the inverted haplotypes in Chr2 not only appear to be more widespread across the common quail distribution range, but we also find no direct evidence of phenotypic effects. Nevertheless, considering that the inverted region on Chr2 spans at least 32 Mbp and contains nearly 290 genes, we cannot rule out the possibility that these are associated with other yet-to-be-identified phenotypic traits.

Chromosomal inversions typically arise locally within single individuals or through introgression, and initially they are susceptible to loss due to genetic drift, deleterious effects at breakpoints, or overall fitness reduction (Faria et al. [2019]). However, if an inversion captures a combination of alleles that enhances fitness or local adaptation under certain environmental conditions, it can increase in frequency because the inversion prevents recombination with non-adaptive variants (Kirkpatrick [2010]). Given the ancient origins of the inversions studied here, dating to more than 1 mya, and their consistent presence in high frequency across diverse geographic localities, it is likely that these inversions are being maintained through balancing selection (see also Ravagni et al. [2024]).

While the suppression of recombination between inverted and non-inverted regions effectively conserves sets of co-adapted alleles, it also predisposes them to the accumulation of deleterious mutations due to inefficient purging (Faria et al. [2019]; Berdan et al. [2021]). In the ancestral state, such mutations would

typically be counter-selected through a mutation-selection-drift balance (Kirkpatrick and Barton 2006). However, diminished selection efficiency from reduced effective population size associated with inversions (Berdan et al. 2023) can lead to an increased genetic load within the inverted haplotypes. This is evident in the higher N/S ratios observed in the inversion regions compared to the rest of the genome (Figure 4), and it is particularly noticeable for the derived rearrangement for Inv1 (BB, Figure 4). In this case, relaxed selection is accentuated by its reduced geographic distribution range, which is further fragmented across the Atlantic archipelagos due to the limited dispersal capability of quails carrying it (Sanchez-Donoso et al. 2022), which further contributes to a lower effective population size. This facilitates a faster accumulation of functional variation across the more than 1200 genes within the inversion, potentially accelerating diversification. Interestingly, the inverted haplotype at Inv1 is found in high frequency in Atlantic archipelagos and appears to have diverged between the archipelagos due to low or nonexistent gene flow between them for this haplotype (see Sanchez-Donoso et al. 2022). Different common quail subspecies have been described across the archipelagos (*C.c. conturbans* for Azores, *C.c. confisa* for Canary Islands and Madeira, *C.c. inopinata* for Cape Verde; del Hoyo et al. 1994; Guyomarc'h and Perennou 2009) and the inversion Inv1 may contribute to their uniqueness (Ravagni et al. 2024). Our findings indicate that geographically restricted inversions may accelerate local adaptation by significantly reducing the effective population size at specific genomic regions. This localised decrease in population size results in a lower purifying selection compared to more broadly distributed haplogroups and a faster accumulation of functional variation.

Our exploration of genes undergoing selection unveiled distinct functional groups prevalent across the inversions. Within Inv1, certain genes could play a role in alterations in migratory behaviour that contribute to the restricted geographical distribution and reduced gene flow across archipelagos of quails carrying the inversion. Genes linked to reproductive processes and molecular signalling suggest potential involvement in modified reproduction and regulatory responses to environmental cues. Additionally, genes related to anatomical structure development and cell differentiation point to broad impacts on quail morphology and physiology, potentially contributing to differences in migratory behaviour. It is plausible that reduced migratory demands in quails with the inversion led to a relaxation in anatomical constraints, fostering a relative accumulation of nonsynonymous substitutions in genes involved in the development of the flight apparatus.

The top genes undergoing selection within Inv2.1 not only exhibit functional parallels with Inv1, involving morphological and cellular alterations, but also play crucial roles in protein modification and enzymatic processes. Their elevated N/S values suggest directional selection. In Inv2.2, the genes with the largest differences in N/S appear more frequently involved in fundamental cellular processes, such as DNA recombination and repair, chromosome segregation, and telomere organisation, which are crucial for genomic stability and maintenance. However, it is not known how these differences would affect individuals with and without the inversion.

Inversions are often hypothesised to accumulate repetitive elements and deleterious variations due to diminished selection pressures (Gutiérrez-Valencia et al. 2021; Jay et al. 2021). Our findings do not show large differences in this regard. For Inv1, inverted haplotypes are slightly shorter, which appears inconsistent with the expectation. It is possible that substantial length discrepancies in large inversions such as this one could interfere with meiotic pairing, potentially resulting in reduced fitness. It is important to note, however, that our *de novo* assembly was based on a quail without the inversion, which may not accurately represent the structure of the inverted haplotype. Further research, including the whole genome sequencing with long-read technology of an individual carrying the inversions, is necessary to determine whether the absence of repetitive sequences is a genuine biological phenomenon or an artefact arising from our methodological approaches.

In conclusion, this study highlights the crucial role of chromosomal inversions in shaping evolutionary forces within specific genome regions. Our findings suggest that inversions, along with other structural variants, might be a significant component of the genome of many species. These variants can exhibit distinct geographic distributions and respond to independent selective pressures, potentially facilitating local adaptation across a species' range. By uncovering the interplay between genomic architecture and evolutionary dynamics, this work contributes to the growing body of evidence that emphasises the importance of structural genomic changes in promoting biodiversity and facilitating adaptation.

Conflicts of Interest

The authors declare no conflicts of interest.

Data Availability Statement

The *de novo* common quail (*Coturnix coturnix*) genome assembly is available on NCBI under the accession number SAMN46992911. The phenotypic data used in this study is provided as Supporting Information (Table S6). Genome sequences of 16 quails and GBS data from Sanchez-Donoso et al. (2022) are deposited in GenBank (GenBank: PRJNA730394) and in https://digital.csic.es/handle/10261/251279 (https://doi.org/10.20350/digitalCSIC/13989).

References

Adams, K. L., and J. F. Wendel. 2005. "Polyploidy and Genome Evolution in Plants." *Current Opinion in Plant Biology* 8: 114–135. https://doi.org/10.1016/j.pbi.2005.01.001.

Alexander, D. H., J. Novembre, and K. Lange. 2009. "Fast Model-Based Estimation of Ancestry in Unrelated Individuals." *Genome Research* 19: 1655–1664. https://doi.org/10.1101/gr.094052.109.

Alonge, M., L. Lebeigle, M. Kirsche, et al. 2022. "Automated Assembly Scaffolding Using RagTag Elevates a New Tomato System for High-Throughput Genome Editing." *Genome Biology* 23: 258. https://doi.org/10.1186/s13059-022-02823-7.

Avril, A., J. Purcell, S. Béniguel, and M. Chapuisat. 2020. "Maternal Effect Killing by a Supergene Controlling Ant Social Organization." *Proceedings of the National Academy of Sciences of the United States of America* 117, no. 29: 17130–17134. https://doi.org/10.1073/pnas.2003282117.

Berdan, E., E. L. Berdan, N. H. Barton, et al. 2023. "How Chromosomal Inversions Reorient the Evolutionary Process." *Journal of Evolutionary Biology* 36, no. 12: 1–22. https://doi.org/10.1111/jeb.14242.

Berdan, E. L., A. Blanckaert, R. K. Butlin, and C. Bank. 2021. "Deleterious Mutation Accumulation and the Long-Term Fate of Chromosomal Inversions." *PLoS Genetics* 17, no. 3: e1009411. https://doi.org/10.1371/journal.pgen.1009411.

Berg, P., B. Star, C. Pampoulie, et al. 2017. "Trans-Oceanic Genomic Divergence of Atlantic Cod Ecotypes Is Associated With Large Inversions." *Heredity* 119: 418–428. https://doi.org/10.1038/hdy.2017.54.

Bohling, J. 2020. "Evaluating the Effect of Reference Genome Divergence on the Analysis of Empirical RADseq Datasets." *Ecology and Evolution* 10: 7585–7601. https://doi.org/10.1002/ece3.6483.

Brelsford, A., J. Purcell, A. Avril, et al. 2020. "An Ancient and Eroded Social Supergene Is Widespread Across Formica Ants." *Current Biology* 30, no. 2: 304–311. https://doi.org/10.1016/j.cub.2019.11.032.

Brown, J. D., and R. J. O'Neill. 2010. "Chromosomes, Conflict, and Epigenetics: Chromosomal Speciation Revisited." *Annual Review of Genomics and Human Genetics* 11, no. 1: 291–316. https://doi.org/10.1146/annurev-genom-082509-141554.

Cáceres, M., J. M. Ranz, A. Barbadilla, M. Long, and A. Ruiz. 1999. "Generation of a Widespread Drosophila Inversion by a Transposable Element." *Science* 285, no. 5426: 415–418. https://doi.org/10.1126/science.285.5426.415.

Challis, R., E. Richards, J. Rajan, G. Cochrane, and M. Blaxter. 2020. "BlobToolKit – Interactive Quality Assessment of Genome Assemblies."

G3 (Bethesda, Md.) 10, no. 4: 1361–1374. https://doi.org/10.1534/g3.119.400908.

Cheng, H., G. T. Concepcion, X. Feng, H. Zhang, and H. Li. 2021. "Haplotype-Resolved de Novo Assembly Using Phased Assembly Graphs With Hifiasm." *Nature Methods* 18: 170–175. https://doi.org/10.1038/s41592-020-01056-5.

Cheng, H., E. D. Jarvis, O. Fedrigo, et al. 2022. "Haplotype-Resolved Assembly of Diploid Genomes Without Parental Data." *Nature Biotechnology* 40: 1332–1335. https://doi.org/10.1038/s41587-022-01261-x.

Christmas, M. J., A. Wallberg, I. Bunikis, A. Olsson, O. Wallerman, and M. T. Webster. 2019. "Chromosomal Inversions Associated With Environmental Adaptation in Honeybees." *Molecular Ecology* 28: 1358–1374. https://doi.org/10.1111/mec.14944.

Dalloul, R. A., J. A. Long, A. V. Zimin, et al. 2010. "Multi-Platform Next-Generation Sequencing of the Domestic Turkey (*Meleagris gallopavo*): Genome Assembly and Analysis." *PLoS Biology* 8, no. 9: e1000475. https://doi.org/10.1371/journal.pbio.1000475.

Danecek, P., A. Auton, G. Abecasis, et al. 2011. "The Variant Call Format and VCFtools." *Bioinformatics* 27: 2156–2158. https://doi.org/10.1093/bioinformatics/btr330.

Danecek, P., J. K. Bonfield, J. Liddle, et al. 2021. "Twelve Years of SAMtools and BCFtools." *GigaScience* 10, no. 2: giab008. https://doi.org/10.1093/gigascience/giab008.

del Hoyo, J., A. Elliott, and J. Sargatal. 1994. *Handbook of the Birds of the World*. Vol. 2. Lynx Edicions.

Elshire, R. J., J. C. Glaubitz, Q. Sun, et al. 2011. "A Robust, Simple Genotyping-Bysequencing (GBS) Approach for High Diversity Species." *PLoS One* 6: e19379. https://doi.org/10.1371/journal.pone.0019379.

Faria, R., K. Johannesson, R. K. Butlin, and A. M. Westram. 2019. "Evolving Inversions." *Trends in Ecology & Evolution* 34: 239–248. https://doi.org/10.1016/j.tree.2018.12.005.

Fuller, Z. L., S. A. Koury, N. Phadnis, and S. W. Schaeffer. 2019. "How Chromosomal Rearrangements Shape Adaptation and Speciation: Case Studies in Drosophila Pseudoobscura and Its Sibling Species *Drosophila persimilis*." *Molecular Ecology* 28: 1283–1301. https://doi.org/10.1111/mec.14923.

Garrison, E., and G. Marth. 2012. "Haplotype-Based Variant Detection From Short-Read Sequencing." arXiv:1207.3907. https://arxiv.org/abs/1207.3907.

Ge, S. X., D. Jung, and R. Yao. 2020. "ShinyGO: A Graphical Gene-Set Enrichment Tool for Animals and Plants." *Bioinformatics* 36, no. 8: 2628–2629. https://doi.org/10.1093/bioinformatics/btz931.

Glaubitz, J. C., T. M. Casstevens, F. Lu, et al. 2014. "TASSEL-GBS: A High Capacity Genotyping by Sequencing Analysis Pipeline." *PLoS One* 9, no. 2: e90346. https://doi.org/10.1371/journal.pone.0090346.

Gray, Y. H. 2000. "It Takes Two Transposons to Tango: Transposable-Element-Mediated Chromosomal Rearrangements." *Trends in Genetics* 16, no. 10: 461–468. https://doi.org/10.1016/s0168-9525(00)02104-1.

Gutiérrez-Valencia, J., P. W. Hughes, E. L. Berdan, and T. Slotte. 2021. "The Genomic Architecture and Evolutionary Fates of Supergenes." *Genome Biology and Evolution* 13, no. 5: evab057. https://doi.org/10.1093/gbe/evab057.

Guyomarc'h, J.-C., and C. Perennou. 2009. "Common quail Coturnix coturnix. European Union Management Plan 2009-2011." Natura 2000. Office for Official Publications of the European Communities, 69 pp.

Harringmeyer, O. S., and H. E. Hoekstra. 2022. "Chromosomal Inversion Polymorphisms Shape the Genomic Landscape of Deer Mice." *Nature Ecology & Evolution* 6: 1965–1979. https://doi.org/10.1038/s41559-022-01890-0.

Hedges, D. J., and P. L. Deininger. 2007. "Inviting Instability: Transposable Elements, Double-Strand Breaks, and the Maintenance of Genome Integrity." *Mutation Research* 616, no. 1–2: 46–59. https://doi.org/10.1016/j.mrfmmm.2006.11.021.

Helleu, Q., C. Roux, K. G. Ross, and L. Keller. 2022. "Radiation and Hybridization Underpin the Spread of the Fire Ant Social Supergene." *Proceedings of the National Academy of Sciences of the United States of America* 119, no. 34: e2201040119. https://doi.org/10.1073/pnas.2201040119.

Höök, L., K. Näsvall, R. Vila, C. Wiklund, and N. Backström. 2023. "High-Density Linkage Maps and Chromosome Level Genome Assemblies Unveil Direction and Frequency of Extensive Structural Rearrangements in Wood White Butterflies (Leptidea Spp.)." *Chromosome Research* 31: 2. https://doi.org/10.1007/s10577-023-09713-z.

Huang, K., K. L. Ostevik, C. Elphinstone, et al. 2022. "Mutation Load in Sunflower Inversions Is Negatively Correlated With Inversion Heterozygosity." *Molecular Biology and Evolution* 39, no. 5: msac101. https://doi.org/10.1093/molbev/msac101.

Hufton, A. L., and G. Panopoulou. 2009. "Polyploidy and Genome Restructuring: A Variety of Outcomes." *Current Opinion in Genetics & Development* 19: 600–606. https://doi.org/10.1016/j.pbi.2005.01.001.

Iijima, T., S. Yoda, and H. Fujiwara. 2019. "The Mimetic Wing Pattern of Papilio Polytes Butterflies Is Regulated by a Doublesex-Orchestrated Gene Network." *Communications Biology* 2: 257. https://doi.org/10.1038/s42003-019-0510-7.

IJdo, J. W., A. Baldini, D. C. Ward, S. T. Reeders, and R. A. Wells. 1991. "Origin of Human Chromosome 2: An Ancestral Telomere-Telomere Fusion." *Proceedings of the National Academy of Sciences of the United States of America* 88, no. 20: 9051–9055. https://doi.org/10.1073/pnas.88.20.9051.

Jay, P., M. Chouteau, A. Whibley, et al. 2021. "Mutation Load at a Mimicry Supergene Sheds New Light on the Evolution of Inversion Polymorphisms." *Nature Genetics* 53: 288–293. https://doi.org/10.1038/s41588-020-00771-1.

Jay, P., A. Whibley, L. Frézal, et al. 2018. "Supergene Evolution Triggered by the Introgression of a Chromosomal Inversion." *Current Biology* 28, no. 11: 1833. https://doi.org/10.1016/j.cub.2018.04.072.

Kartout-Benmessaoud, Y., and K. Ladjali-Mohammedi. 2018. "Banding Cytogenetics of Chimeric Hybrids *Coturnix coturnix* × Coturnix Japonica and Comparative Analysis With the Domestic Fowl." *Comparative Cytogenetics* 12, no. 4: 445–470. https://doi.org/10.3897/CompCytogen.v12i4.27341.

Kartout-Benmessaoud, Y., S. Ouchia-Benissad, L. Mahiddine-Aoudjit, and K. Ladjali-Mohammedi. 2024. "Highlighting Chromosomal Rearrangements of Five Species of Galliformes (Domestic Fowl, Common and Japanese Quail, Barbary and Chukar Partridge) and the Houbara Bustard, an Endangered Otidiformes: Banding Cytogenetic Is a Powerful Tool." *Comparative Cytogenetics* 18: 213–237. https://doi.org/10.3897/compcytogen.18.135056.

Katoh, K., and D. M. Standley. 2013. "MAFFT Multiple Sequence Alignment Software Version 7: Improvements in Performance and Usability." *Molecular Biology and Evolution* 30, no. 4: 772–780. https://doi.org/10.1093/molbev/mst010.

Kirkpatrick, M. 2010. "How and Why Chromosome Inversions Evolve." *PLoS Biology* 8: e1000501. https://doi.org/10.1371/journal.pbio.1000501.

Kirkpatrick, M., and N. Barton. 2006. "Chromosome Inversions, Local Adaptation and Speciation." *Genetics* 173: 419–434. https://doi.org/10.1534/genetics.105.047985.

Kopelman, N. M., J. Mayzel, M. Jakobsson, N. A. Rosenberg, and I. Mayrose. 2015. "Clumpak: A Program for Identifying Clustering Modes and Packaging Population Structure Inferences Across K." *Molecular Ecology Resources* 15: 1179–1191. https://doi.org/10.1111/1755-0998.12387.

Korunes, K. L., and M. A. F. Noor. 2019. "Pervasive Gene Conversion in Chromosomal Inversion Heterozygotes." *Molecular Ecology* 28: 1302–1315. https://doi.org/10.1111/mec.14921.

Labocha, M. K., and J. P. Hayes. 2012. "Morphometric Indices of Body Condition in Birds: A Review." *Journal of Ornithology* 153: 1–22. https://doi.org/10.1007/s10336-011-0706-1.

Lamichhaney, S., G. Fan, F. Widemo, et al. 2016. "Structural Genomic Changes Underlie Alternative Reproductive Strategies in the Ruff (*Philomachus pugnax*)." *Nature Genetics* 48: 84–88. https://doi.org/10.1038/ng.3430.

Langmead, B., and S. Salzberg. 2012. "Fast Gapped-Read Alignment With Bowtie 2." *Nature Methods* 9: 357–359. https://doi.org/10.1038/nmeth.1923.

Li, H. 2011. "A Statistical Framework for SNP Calling, Mutation Discovery, Association Mapping and Population Genetical Parameter Estimation From Sequencing Data." *Bioinformatics* 27, no. 21: 2987–2993. https://doi.org/10.1093/bioinformatics/btr509.

Li, H., and R. Durbin. 2009. "Fast and Accurate Short Read Alignment With Burrows-Wheeler Transform." *Bioinformatics* 25: 1754–1760. https://doi.org/10.1093/bioinformatics/btp324.

Lohse, K., M. Clarke, M. G. Ritchie, and W. J. Etges. 2015. "Genome-Wide Tests for Introgression Between Cactophilic Drosophila Implicate a Role of Inversions During Speciation." *Evolution* 69, no. 5: 1178–1190. https://doi.org/10.1111/evo.12650.

Lundberg, M., A. Mackintosh, A. Petri, and S. Bensch. 2023. "Inversions Maintain Differences Between Migratory Phenotypes of a Songbird." *Nature Communications* 14: 452. https://doi.org/10.1038/s41467-023-36167-y.

Maney, D., J. Merritt, M. Prichard, B. Horton, and S. Yi. 2020. "Inside the Supergene of the Bird With Four Sexes." *Hormones and Behavior* 126: 104850. https://doi.org/10.1016/j.yhbeh.2020.104850.

Matschiner, M., J. M. I. Barth, O. K. Tørresen, et al. 2022. "Supergene Origin and Maintenance in Atlantic Cod." *Nature Ecology & Evolution* 6: 469–481. https://doi.org/10.1038/s41559-022-01661-x.

McKenna, A., M. Hanna, E. Banks, et al. 2010. "The Genome Analysis Toolkit: A MapReduce Framework for Analyzing Next-Generation DNA Sequencing Data." *Genome Research* 20: 1297–1303. https://doi.org/10.1101/gr.107524.110.

McLaren, W., L. Gil, S. E. Hunt, et al. 2016. "The Ensembl Variant Effect Predictor." *Genome Biology* 17: 122. https://doi.org/10.1186/s13059-016-0974-4.

Mérot, C., R. A. Oomen, A. Tigano, and M. Wellenreuther. 2020. "A Roadmap for Understanding the Evolutionary Significance of Structural Genomic Variation." *Trends in Ecology & Evolution* 35, no. 7: 561–572. https://doi.org/10.1016/j.tree.2020.03.002.

Morris, K. M., M. M. Hindle, S. Boitard, et al. 2020. "The Quail Genome: Insights Into Social Behaviour, Seasonal Biology and Infectious Disease Response." *BMC Biology* 18: 14. https://doi.org/10.1186/s12915-020-0743-4.

Nam, K., C. Mugal, B. Nabholz, et al. 2010. "Molecular Evolution of Genes in Avian Genomes." *Genome Biology* 11: R68. https://doi.org/10.1186/gb-2010-11-6-r68.

Nishikawa, H., T. Iijima, R. Kajitani, et al. 2015. "A Genetic Mechanism for Female-Limited Batesian Mimicry in Papilio Butterfly." *Nature Genetics* 47: 405–409. https://doi.org/10.1038/ng.3241.

Pérez-Wohlfeil, E., S. Diaz-del-Pino, and O. Trelles. 2019. "Ultra-fast genome comparison for large-scale genomic experiments." *Scientific Reports* 9, no. 1: 1–10. https://doi.org/10.1038/s41598-019-46773-w.

Pockrandt, C., M. Alzamel, C. S. Iliopoulos, and K. Reinert. 2020. "GenMap: Ultra-Fast Computation of Genome Mappability." *Bioinformatics* 36, no. 12: 3687–3692. https://doi.org/10.1093/bioinformatics/btaa222.

Poszewiecka, B., K. Gogolewski, P. Stankiewicz, and A. Gambin. 2022. "Revised Time Estimation of the Ancestral Human Chromosome 2 Fusion." *BMC Genomics* 23, no. 6: 616. https://doi.org/10.1186/s12864-022-08828-7.

Puigcerver, M., S. Gallego, J. D. Rodríguez-Teijeiro, and J. C. Senar. 1992. "Survival and Mean Life Span of the Quail Coturnix c. Coturnix." *Bird Study* 39: 120–123. https://doi.org/10.1080/00063659209477108.

Quinlan, A. R., and I. M. Hall. 2010. "BEDTools: A Flexible Suite of Utilities for Comparing Genomic Features." *Bioinformatics* 26, no. 6: 841–842. https://doi.org/10.1093/bioinformatics/btq033.

R Core Team. 2022. "R: A Language and Environment for Statistical Computing." R Foundation for Statistical Computing. Retrieved from. https://www.R-project.org/.

Ravagni, S., I. Sanchez-Donoso, I. Jiménez-Blasco, et al. 2024. "Evolutionary History of an Island Endemic, the Azorean Common Quail." *Molecular Ecology* 33, no. 24: e16997. https://doi.org/10.1111/mec.16997.

Rieseberg, L. H. 2001. "Chromosomal Rearrangements and Speciation." *Trends in Ecology & Evolution* 16: 351–358. https://doi.org/10.1016/S0169-5347(01)02187-5.

RStudio Team. 2022. "RStudio: Integrated Development Environment for R." RStudio, PBC. Retrieved from. http://www.rstudio.com/.

RStudio Team. 2023. "RStudio: Integrated Development Environment for R." RStudio, PBC. Retrieved from. http://www.rstudio.com/.

Sanchez-Donoso, I., S. Ravagni, J. D. Rodríguez-Teijeiro, et al. 2022. "Massive Genome Inversion Drives Coexistence of Divergent Morphs in Common Quails." *Current Biology* 32, no. 2: 462–469.e6. https://doi.org/10.1016/j.cub.2021.11.019.

Sanchez-Flores, A., F. Peñaloza, J. Carpinteyro-Ponce, et al. 2016. "Genome Evolution in Three Species of Cactophilic Drosophila." *G3 (Bethesda, Md.)* 6, no. 10: 3097–3105. https://doi.org/10.1534/g3.116.033779.

Santiago, E., I. Novo, A. F. Pardiñas, M. Saura, J. Wang, and A. Caballero. 2020. "Recent Demographic History Inferred by High-Resolution Analysis of Linkage Disequilibrium." *Molecular Biology and Evolution* 37, no. 12: 3642–3653. https://doi.org/10.1093/molbev/msaa169.

Shin, J., S. Blay, B. McNeney, and J. Graham. 2006. "LDheatmap: An R Function for Graphical Display of Pairwise Linkage Disequilibria Between Single Nucleotide Polymorphisms." *Journal of Statistical Software, Code Snippet* 16: 1–9. https://doi.org/10.18637/jss.v016.c03.

Schwander, T., R. Libbrecht, and L. Keller. 2014. "Supergenes and Complex Phenotypes." *Current Biology* 24, no. 7: R288–R294. https://doi.org/10.1016/j.cub.2014.01.056.

Shumate, A., and S. L. Salzberg. 2021. "Liftoff: Accurate Mapping of Gene Annotations." *Bioinformatics* 37, no. 12: 1639–1643. https://doi.org/10.1093/bioinformatics/btaa1016.

Smeds, L., A. Qvarnström, and H. Ellegren. 2016. "Direct Estimate of the Rate of Germline Mutation in a Bird." *Genome Research* 26, no. 9: 1211–1218. https://doi.org/10.1101/gr.204669.116.

Smit, A. F. A., R. Hubley, and P. Green. 2013. "RepeatMasker Open-4.0." http://www.repeatmasker.org.

Stein, R. W., J. W. Brown, and A. Ø. Mooers. 2015. "A Molecular Genetic Time Scale Demonstrates Cretaceous Origins and Multiple Diversification Rate Shifts Within the Order Galliformes (Aves)." *Molecular Phylogenetics and Evolution* 92: 155–164. https://doi.org/10.1016/j.ympev.2015.06.005.

Thompson, M. J., and C. D. Jiggins. 2014. "Supergenes and Their Role in Evolution." *Heredity* 113, no. 1: 1–8. https://doi.org/10.1038/hdy.2014.20.

Tuttle, E. M., A. O. Bergland, M. L. Korody, et al. 2016. "Divergence and Functional Degradation of a Sex Chromosome-Like Supergene." *Current Biology* 26: 344–350. https://doi.org/10.1016/j.cub.2015.11.069.

Wang, J., Y. Wurm, M. Nipitwattanaphon, et al. 2013. "A Y-Like Social Chromosome Causes Alternative Colony Organization in Fire Ants." *Nature* 493, no. 7434: 664–668. https://doi.org/10.1038/nature11832.

Wellenreuther, M., and L. Bernatchez. 2018. "Eco-Evolutionary Genomics of Chromosomal Inversions." *Trends in Ecology & Evolution* 33, no. 6: 427–440. https://doi.org/10.1016/j.tree.2018.04.002.

Wellenreuther, M., C. Mérot, E. Berdan, and L. Bernatchez. 2019. "Going Beyond SNPs: The Role of Structural Genomic Variants in Adaptive Evolution and Species Diversification." *Molecular Ecology* 28: 1203–1209. https://doi.org/10.1111/mec.15066.

Wickham, H. 2009. *ggplot2: Elegant Graphics for Data Analysis*. Springer-Verlag. https://ggplot2.tidyverse.org.

Yunis, J. J., and O. Prakash. 1982. "The Origin of Man: A Chromosomal Pictorial Legacy." *Science* 215, no. 4539: 1525–1530. https://doi.org/10.1126/science.7063861.

Zheng, X., D. Levine, J. Shen, S. M. Gogarten, C. Laurie, and B. S. Weir. 2012. "A High-Performance Computing Toolset for Relatedness and Principal Component Analysis of SNP Data." *Bioinformatics* 28: 3326–3328. https://doi.org/10.1093/bioinformatics/bts606.

Supporting Information

Additional supporting information can be found online in the Supporting Information section.